THE INDUCTION OF THE OPTIC FLOW MOTION AFTEREFFECT IN THE CENTRAL VERSUS PERIPHERAL VISUAL FIELD

By

LISA MARIE TRIPP

A thesis submitted in partial fulfillment of
the requirements for the degree of

MASTER OF SCIENCE IN PSYCHOLOGY

WASHINGTON STATE UNIVERSITY

Department of Psychology

DECEMBER 2009

To the Faculty of Washington State University:

The members of the Committee appointed to examine the thesis of LISA MARIE TRIPP find it satisfactory and recommend that it be accepted.

_____

Robert Patterson, Ph.D. Chair

_____

Bala Krishnamoorthy, Ph.D.

_____

Lisa Fournier, Ph.D.

THE CENTRAL VERSUS PERIPHERAL VISUAL FIELD AND INDUCTION OF THE OPTIC FLOW MOTION AFTEREFFECT

Abstract

by Lisa Marie Tripp, M.S.
Washington State University
December 2009

Chair: Robert Patterson

One remarkable phenomenon reported in the literature on motion perception is called the motion aftereffect (MAE), which refers to the illusion of motion in a given direction following adaptation to real motion in the opposite direction. The purpose of the present study was to investigate the induction of the MAE using an optic flow motion stimulus, which was created from simulated self-movement through a real-world perspective scene. Specifically, the effect of adaptation using the central versus peripheral visual field on the duration of the optic flow MAE was investigated. In doing so, the areas of the central versus peripheral adapting stimulus were equated by scaling for cortical magnification. Results showed that the duration of the MAE was shorter when the adapting optic flow motion was presented in the peripheral visual field than when it was presented centrally. These results were interpreted as reflecting a more transient response in the automatic gain control mechanisms in the motion pathways projecting from the peripheral retina.

TABLE OF CONTENTS

Page

ABSTRACT……..iii

LIST OF FIGURES……..iv

SECTIONS

1. INTRODUCTION……6
2. RESEARCH METHODOLOGY…….……....14
3. RESULTS ..……...…….....17
4. DISCUSSION…….….18

REFERENCES……...…….28

APPENDIX……..33

LIST OF FIGURES

1. Simulated Real-World Scene……..……34

2. Test Stimuli…….…...…35

3. MAE Duration for three adapting speeds and three viewing conditions……..…..36

4. System Dynamics Representation of the SRW Optic Flow MAE Model…...….....37

SECTION ONE
INTRODUCTION

The ability to perceive motion in the environment is imperative to the survival of animals, including humans. Motion perception is essential so that we can quickly detect and evade predators as well as inanimate objects that may strike us. For example, crossing a busy street relies heavily upon our ability to detect and process motion information. Besides obstacle avoidance, motion perception is also important for all types of locomotion, from very simple tasks such as a toddler walking a couple steps towards a toy to more complex tasks that require some type of specialized training such as driving an automobile. In such tasks, moving around a complex environment requires the ability to perceive the velocity of both ourselves and of other moving stimuli.

One remarkable phenomenon reported in the literature on motion perception is called the motion aftereffect (MAE). The MAE occurs when an individual views real motion in a given direction for a period of time. During the viewing of the motion, perceptual adaptation occurs. When the motion stops, the individual will typically experience an illusion of motion in the opposite direction. The motion aftereffect is a visual illusion that has become an important tool for studying the properties of stages of motion processing in the visual system. For example, the MAE has been used to identify lower processing levels of the motion stream that process temporal rates of change (Pantle, 1974), as well as higher levels that process stimulus velocity (e.g., Nishida & Sato, 1995). Additionally, the MAE has been used to explore the role of attention in motion processing (Chaudhuri, 1990; Patterson, Fournier, Wiediger, Vavrek, Becker-Dippman, & Bickler, 2005).

Although interesting, most studies of the MAE have been limited in terms of the type of stimuli used to induce the illusion of motion. For example, studies have used one-dimensional grating patterns (e.g., Bex, Metha, & Makous, 1999), two dimensional plaid patterns (e.g., Burke & Wenderoth, 1993), or rotating spiral patterns (e.g., Cavanagh & Favreau, 1980) as the adapting stimulus. In these cases, such stimuli are devoid of many, if not most, of the naturally-occurring cues encountered when an observer interacts with his or her environment.

For example, rotating patterns contain a subset of cues (e.g., expansion information) used in locomotion and the control of self-motion. However, even spiral patterns are very limited because they are presented on a flat planar surface (e.g., computer screen). In general, typical studies of the MAE have not employed dynamic scenes in perspective view, the z-axis depth of which would yield strong optic flow information. Optic flow (see Gibson, 1937; Warren, 1998) refers to the global flow field of relative motion information that is generated when an observer translates in the forward direction while locomoting through the world. Such optic flow information would contain rich motion parallax cues, which refers to differential motion of retinal images coming from objects located at different depths. The motion parallax information contained in optic flow is an important cue for inducing the sense of self-movement through space (Patterson, Tripp, Rogers, & Boydstun, 2009). An important research issue, then, is to investigate the induction of MAE in the context of self-motion through a real-world scene composed of perspective cues and strong motion parallax.

The purpose of the present study is to investigate the induction of the MAE using optic flow containing motion parallax information as an adapting stimulus, which we call the simulated real world (SRW) MAE. In a previous study, simulated self-movement over a real-world perspective scene was utilized as a stimulus by Patterson et al. (2009). These authors

showed that very robust SRW MAEs can be generated by adaptation to this kind of optic flow stimulus. The results from that study were interpreted within the context of neural processing at levels of the motion stream representing self-motion through external space (Bremmer, 2006; Bremmer, 2005; Bremmer et al., 2002; Bremmer et al., 1997).

One intriguing question about the optic flow MAE is whether stimulation in the periphery versus in the central visual field is required to induce the effect. Traditionally, many authors have assumed that the sense of self-motion, as well as other forms of body orientation and alignment, is primarily mediated by stimulation in the periphery. For example, Brant, Dichgans, and Koenig (1973) studied circular vection, the illusion of self-motion, which was created by using circular disks positioned at an eccentricity ranging from 45 to 75 degrees. Brant et al. found that stimulation in the peripheral visual field (75 degrees eccentricity) alone was sufficient to obtain vection, an effect that declined with decreasing eccentricity. Additional research in linear and roll vection supported Brant et al. (Held, Dishgans, & Bauer, 1975; Berthoz, Pavard, & Young, 1977). Early research into postural adjustments also suggested that the peripheral visual field plays a strong role in the sense of body orientation. For example, a study by Lestiene, Soechting, and Berthoz (1977) found that occlusion of the peripheral visual field led to increased sway relative to occlusion of the central visual field.

However, more recent research has demonstrated that similar, and sometimes stronger, effects related to vection and body orientation occur when only the central visual field is stimulated. For example, Anderson (1986) showed that linear vection occurred with stimulation of the central visual field with areas as small as 7.5 degrees in diameter (see also Andersen & Braunstein, 1985). Moreover, Howard and Heckman (1989) found that circular vection was

strong with stimulation of the central visual field using an area whose diameter that measured 13.5 degrees. Recent studies in postural adjustment also call into question the peripheral-field dominance hypothesis. For example, Palus, Straube, and Brandt (1984) showed no difference in body sway with a 30-degree central visual field compared with a full peripheral visual field. Furthermore, studies examining whether the peripheral or central visual field is dominant in heading judgments also show a significant role for central vision. Warren (1992) studied whether the perceived direction of self-motion was more accurate when peripheral vision or central vision was occluded, with peripheral vision defined as a magnitude of eccentricity ranging from 10 to 40 degrees and central vision defined as a disked-shaped region with a diameter ranging from 10 to 25 degrees. Warren found that, contrary to the peripheral-field dominance hypothesis, heading judgments were more accurate with central vision than with peripheral vision, with accuracy decreasing as eccentricity increased. This pattern of results indicated that the peripheral visual field is less sensitive to optic flow patterns. Warren (1992) argued that studies which supported the peripheral-field dominance hypothesis in the past employed stimuli whose central and peripheral areas were not equated for retinal size.

Several studies of the motion aftereffect using simple adapting patterns have examined the influence of stimulation in the central versus peripheral visual field. These MAE studies have also found conflicting evidence that could be attributed to stimulus size. For example, O'Shea et al. (1994) had participants adapt to a spiral pattern configured as a small circular disk (diameter of 2.8 degrees) or a larger annulus (internal diameter of 40 degrees and external diameter of 80 degrees). The results revealed that the MAE induced in the central visual field were greater than that induced in the peripheral visual field.

In contrast, several recent studies have shown stronger MAEs in the periphery. For example, Castet, Keeble, and Verstraten (2002) had observers adapt to dynamic random-dot stimuli using a 4 x 4 square degree aperture located at an eccentricity of 0, 4, or 7 degrees. The results showed that the strength of the MAE increased with increasing eccentricity. In another study, Price, Greenwood, and Ibbotson (2004) had participants adapt to a spiral pattern that was either a small central annulus (inner radius 0.5 degrees and outer radius 5 degrees) or a larger annulus (inner diameter 5 degrees and an outer diameter 7 degrees). Price et al. found that the magnitude of the MAE was stronger with the peripheral stimulus as compared with the central stimulus.

In summary, although early studies suggested that the peripheral visual field played an important role in the sense of self-motion and body orientation and alignment, more recent studies have suggested that the central visual field plays a key role in those phenomena. Studies of the MAE are also conflicted, with an early study showing that the central visual field plays an important role in the induction of the MAE, but later studies suggested that the peripheral visual field plays a key role. Importantly, all of these studies contained methodological flaws in that the relative size of the area of the central and peripheral stimulation were not equated (O'Shea et al., 1994; Warren, 1992).

Importantly, when comparing the central versus the peripheral visual field and their influence on visual processing, one must take into account the concept of cortical magnification. Cortical magnification refers to the progressive change in the amount of tissue devoted to neural processing in the anatomical projections from the retina to the cortex. Specifically, the central area of the retina becomes significantly magnified, at the expense of the visual periphery, in the

projections reaching the cortex (Virsu & Rovamo, 1978; Rovamo & Virsu, 1978; Levi, Klein, & Aitsebamo, 1985). Thus, for any visual function dependent upon cortical processing, a comparison between central and peripheral stimulation must equate their areas at the cortical level of processing by taking into account the cortical magnification factor. Because in humans motion information is processed at cortical levels of the visual system (Blake & Sekuler, 2005), any comparison of central versus peripheral stimulation must involve stimuli scaled for cortical magnification which would equate their cortical areas activated by stimulation.

The topic of cortical magnification has attracted considerable attention over the years, and thus there has been some variability in the values reported in the literature (Cowey & Rolls, 1974; Dow et al., 1985). One can derive an estimate based on anatomical considerations as well as considering how basic visual functions such as hyperacuity, relative motion and absolute motion processing, vary with eccentricity. According to Levi et al. (1985), a stimulus positioned at an eccentricity of 9-10 degrees should be a factor of 12 times larger than a centrally positioned stimulus (see Levi et al. Figure 12). The Levi et al. study used a hyperacuity task known as a vernier acuity task to study performance in the central visual field versus performance in the peripheral visual field. Levi et al. found that performance declined with increasing eccentricity. They found that the rate of decline was consistent with physiological data on cortical magnification. These authors discovered that, when cortical magnification was considered, performance on the hyperacuity tasks was the same foveally as peripherally.

With respect to the MAE, we are aware of only one study, by Murakami and Shimojo (1995), that considered cortical magnification. These authors examined the effects of stimulus size and eccentricity on the duration of the MAE by using a surrounding pattern composed of a

one-dimensional grating whose dimensions measured 23.5 degrees (H) by 17.6 degrees (V), which contained a center area that varied in diameter and eccentricity. The surrounding pattern moved either in the same direction as the center area, in the opposite direction, or was stationary, during adaptation. The results showed that the factors of stimulus size and eccentricity strongly interacted: at a small eccentricity (e.g., 3 degrees), MAE duration increased with increasing stimulus size, but at large eccentricities (e.g., 10.5 degrees), MAE duration decreased with increasing size. More important for present purposes, this study by Murakami and Shimojo gives us information about cortical magnification. These authors found that when the peripheral stimulus whose eccentricity was 10.5 degrees was scaled in size by a factor of 10-12 relative to the central stimulus, their MAE data could be accounted for at various eccentricities.

Therefore, the present study will investigate the role of the central versus peripheral visual field in the induction of the SRW MAE by taking into account the cortical magnification factor, as revealed in both the Levi et al. and Murakami and Shimojo studies, when designing our stimuli. Based on recent research on self-motion, the results of which contradict the peripheral-field dominance hypothesis (Anderson, 1986; Andersen & Braunstein, 1985; Howard & Heckman, 1989; Palus, Straube, & Brandt, 1984; Warren, 1992), and also on the results of the O'Shea et al. (1994) study of the MAE, I predict that the duration of the motion aftereffect will be longer for the stimuli in the central visual field versus the peripheral visual field when cortical magnification is taken into account. Such a result would be interpreted a more sustained response in the automatic gain control mechanisms in the motion pathways projecting from the central retina relative to the peripheral retina, a topic which is discussed in the Results and Discussion section later in this paper.

A second factor of interest is the speed of simulated self-motion used for adaptation. For other MAE stimuli, such as moving random-dot arrays, variations in the velocity of adapting motion typically result in changes in the duration of the MAE that follow an inverted-U-shaped function: maximal MAE duration occurs with moderate adapting speed (Wohlgemuth, 1911; Granit, 1928; Scott & Noland, 1965, Thompson, 1993). Presumably the changes in MAE duration with variation in adapting speed reflects a shift in the activity across subpopulations of motion-processing cells, with some cells selective for relatively slow motion speeds and other cells selective for faster motion speeds (Verstraten, der Smagt, & van de Grind, 1998); the cells selective for intermediate speeds would be generating the longer MAEs. The question remains as to whether an analogous relationship occurs between adaptation speed and MAE duration when simulated self-motion is used as the adapting stimulus.

SECTION TWO

RESEARCH METHODOLOGY

Observers

Eleven observers participated**.** All observers had normal or corrected-to-normal acuity in each eye, normal binocular vision, normal color vision, and normal phoria (tested with an Ortho-rater, Bausch & Lomb, Chicago, IL). All observers gave documented informed consent.

Stimuli and Apparatus

Terrain imagery was displayed on a 36-inch monitor, whose dimensions were 27.5 arcdeg (height) x 35.2 arcdeg (width) and were viewed from a distance of 114 cm. The terrain imagery appeared as a flat gray ground plane in perspective view which was populated by a large number of vertically-oriented poles. Pole density was 576 poles/m^2. In the simulation, the size of each pole was 7m tall by 1m wide. The visual angle of the closest poles was 7.5 deg (height) X 0.5 deg (width) and for the farthest poles it was 0.5 deg (height) X 0.05 deg (width). The poles provided object perspective, motion parallax close to eye level, dynamic occlusion and disclosure, and multiple reference objects. A horizon was clearly visible in the distance. The average luminance of the scenes ranged from 41.7 to 48.9 cd/m^2, depending upon condition. The terrain imagery was generated using commercial database development software (World Perfect 2.0, MetaVR, Brookline, MA). Travel over the terrain was simulated using a PC-based runtime system (Virtual Reality Scene Generator, MetaVR).

The central and peripheral adapting stimuli were created by masking off selected portions of the display using cardboard whose average luminance was approximately the same as that of the display. In doing so, the stimuli were scaled for cortical magnification. The area of the peripheral stimulus was a factor of 12 times larger than the area of the central stimulus (see Levi, Klein, & Aitsebamo, 1985, Figure 12; Murakami & Shimojo, 1995, Figure 7). The peripheral stimulus was configured as a surrounding annular-shaped patch of terrain and poles whose mid-point was located at an eccentricity of 9 degrees in all radial directions. The central area was configured as a central disk-shaped patch of terrain and poles located at an eccentricity of zero degrees. The central disk had a radius 3.84 degrees and an area of 46.30 square degrees. The peripheral annulus had an external radius of 13.66 degrees and internal radius of 3.84 degrees, and an area of 540.01 square degrees. The speed of adapting optic flow motion (e.g., global optical flow rate) was 10, 20, or 40 eyeheights/sec (25, 50, or 100 m/sec), and simulated altitude was 2.5 m.

Procedure

The design of this study was a 3 (viewing condition: central stimulation, peripheral stimulation, and baseline stimulation) x 3 (speed of simulated self-movement: 10, 20, or 40 eyeheights/sec) within-subjects factorial design. During each trial, the observer was instructed to fixate the center of the display screen and experience simulated forward motion at a given speed of simulated travel (e.g., global optic flow rate). Because the simulated self motion entailed forward translation, the optic flow involved elements in the scene near fixation moving expansively outward toward the periphery such that an expansive flow field was created. This expansive flow field would assist the observers in maintaining fixation on the central fixation point because the individual motion vectors would have been balanced around the fixation point.

This would not have been true for, say, simple gratings patterns moving leftward or rightward for which the tendency for tracking eye movements in a given direction would have been greater. Thus, the control of fixation in our study allowed us to interpret the results in terms of central versus peripheral retinal areas. The observer adapted to the resulting optic flow for a duration of adaptation of 1 minute. At the end of adaptation, the simulated travel abruptly stopped and the scene became static, which began the test phase (e.g., the last scene served as the stationary test pattern). Thus, the adapting stimulus and the test stimulus had the same dimensions and visual field location. During the test phase, the observer experienced the aftereffect as a visual illusion of sensed backward movement. The observer verbally signaled the end of the aftereffect by saying “stop”; the duration of the aftereffect was be measured with a stop watch and immediately recorded by the experimenter. Four trials were collected under each condition for each observer.

SECTION THREE

RESULTS

The MAE duration times from four trials under each condition for each observer were averaged together to provide an estimate of the duration of the MAE under each condition for each of the 11 observers. These estimates were averaged together across the 11 observers to provide a mean MAE duration for each condition.

Figure 3 depicts the MAE duration for three different adapting speeds and three viewing conditions, shown as parameter. The figure shows that MAE duration increased slightly with increased adapting speeds. Furthermore, the figure shows that MAE duration was largest under the baseline condition. The next largest MAE durations were from the central condition and the smallest from the peripheral condition.

These data were statistically analyzed by computing an analysis of variance for within-subjects designs. This analysis revealed both significant main effects. Viewing condition was significant, $F(2,20) = 5.194$, $p = .015$. Post hoc testing using Fisher's Least Significant Difference (LSD) revealed that only the duration of the peripheral MAE was significantly less than the duration of the baseline condition ($p = .003$). This indicates that the duration of a typical baseline MAE induced with a full field of view could be fully accounted for by central stimulation. This analysis also showed a main effect of adapting speed ($F(2,20) = 5.046$, $p = .043$) (using Greenhouse-Geisser correction). Post hoc testing using Fisher's LSD revealed that 10 eyeheights/s had significantly shorter MAE duration than both 20 and 40 eyeheights/s ($p = .026$ and $p = .044$, respectively). There was no significant interaction between viewing condition and adapting speed ($F(4,40) = 1.676$, $p = .175$).

SECTION FOUR

DISCUSSION

This study investigated the effect of the eccentricity of the adapting stimulus (e.g., viewing condition) and of global optical flow rate (e.g., simulated translation speed) on the duration of the simulated real-world (SRW) optic flow motion aftereffect (MAE). The results showed that viewing condition significantly influenced the duration of the SRW optic flow MAE. Specifically, when the sizes of the central and peripheral stimulus were scaled for cortical magnification, the duration of the SRW MAE in the periphery was significantly shorter than the MAE in the baseline condition. Additionally, the speed of global optical flow rate also significantly influenced the duration of the SRW optic flow MAE such the faster speeds resulted in longer MAE durations.

In interpreting these results, first note that the MAE has been modeled as reflecting the operation of an automatic gain control mechanism in the visual system (van de Grind et al., 2003; van de Grind et al 2004; Patterson et al., 2009). According to this idea, adaptation to motion decreases the responsiveness of neurons tuned to the direction of adapting motion via modulation of an automatic gain control mechanism located in the pathways activated by the adapting motion. The selective lowering of the gain in the adapted pathways produces an imbalance of activity across networks of directionally-selective neurons when a stationary test pattern is viewed, leading to the perception of illusory motion in the opposite direction (e.g., the MAE). This illusion of motion is thought to end when the network of neurons regains it equilibrium.

The purpose of these automatic gain control mechanisms is to shift the operating range of the system to match the current level of stimulation (Lankheet, van Wezel, & van de Grind, 1991). During adaptation, the level of stimulation is high, and the system via the gain control mechanisms lowers its sensitivity (e.g., the operating range shifts to higher stimulus levels) so that differences between levels of stimulation at the high end of the continuum can be differentially represented. In other words, the system shifts its operating range during adaptation to higher levels of stimulation to match the adapting stimulus. In a sense, automatic gain control serves to introduce a degree of plasticity into a system that must respond to large variations in stimulation throughout the environment. Therefore, these results, which indicate that the peripheral retina produces a relatively shorter MAE duration, suggest that the peripheral retina possesses a faster response when adjusting its automatic gain control than does the central retina.

Recently, this gain control process has been modeled by Patterson et al. (2009) by employing a system dynamics framework (see Figure 4). System dynamics is a set of modeling techniques that describe a dynamical system in terms of interconnected components. These components are broken down into classes: stocks are used to represent integrators, flows represent derivatives, and converters represent variables, constants, and conditional expressions. Through the interconnection of sets of these components, systems of differential equations can be simulated. These systems of differential equations are solved via a step-wise numerical-integration technique.

The system dynamics model of gain control by Patterson et al. was based on van de Grind et al.'s (2003, 2004) basic model. This basic model was simplified by having only two opponent motion-direction channels, a ‘forward’ channel and a 'backward' channel in the context of an optic flow stimulus. The forward channel was assumed to be the one being adapted. During

adaptation, stimulation induced a 'charge' in a corresponding leaky integrator, which accumulated over time. Accumulation of the charge affected system responding by inhibiting signal output in the affected channel, an inhibitory effect that was represented as a division. A lowered gain in the adapted channel gave it a lower output during testing relative to the non-adapted channel. During testing, the non-adapted channel was most active, which produced an illusion of motion in the direction signaled by the non-adapted channel. The MAE ended when the difference between the output of the adapted and non-adapted channels became less than a perceptual criterion θ.

The output of each channel was expressed as:

$$channel\ output = y(t_s) = \frac{x(t_s)}{(1+u(t_s))} \quad (1)$$

where $x(t_s)$ was the stimulation over time since the start of the simulation, and the denominator, $(1+u(t_s))$, was the expression for the automatic gain control, e.g. the gain control was expressed as: $gain = 1/(1+u(t_s))$, where $u(t_s)$ was defined as either $u_f(t_s)$ *or* $u_b(t_s)$.

Adaptation selectively produced a charge in the leaky integrator that responded to the direction of the adapting stimulus:

$$adapting\ charge = wx_a(1-e^{-kt_a}) \quad (2)$$

where x_a was the adapting stimulus, w was a weighting factor, t_a was the time spent adapting, and k was the inverse of the time constant. This expression for the adapting charge produced a quickly accelerating and quickly saturating function, called an RC circuit response.

During the test phase, the charge built up during adaptation began to leak according to an exponential decay; that is, the charge built up from adaptation decayed only when the adapting stimulus was removed and testing began. (Note that during the test phase, the charge built up from testing did not decay because the test stimulus was always present during the test phase.) Thus,

$$decay\ of\ adapting\ charge = e^{-kt} \tag{3}$$

where t refers to the time spent testing.

In Patterson et al.'s system dynamics implementation of the model (Figure 4), they had a weighted stimulus that provided constant input to the leaky integrator during the adapt and test phase,

$$adapting\ charge = wx_ak; \tag{4}$$

$$testing\ charge = wx_tk; \tag{5}$$

where x_a and x_t referred to the adapting stimulus and test stimulus, respectively, w was a weighting factor, and k was the inverse of the time constant. The charge being built up during adaptation, as well as the charge being built up during testing, was always continuously leaking according to an exponential decay function:

$$\textit{decay of adapting or test charge} = e^{-kt_s} \quad (6)$$

where t_s indicated the time spent since the beginning of the simulation. When the leaky integrator integrated the difference between input and output, these expressions reduced to the original RC circuit response in the van de Grind et al. model (for more detail, see Appendix B in Patterson et al., 2009). And when the adapting stimulus was eventually removed and replaced by the test stimulus, the charge in the adapted leaky integrator decayed because the test stimulus was weak relative to the decay rate.

The gain in each of the two motion-direction channels was denoted by the symbol *g*. The inverse of the time constant of the negative feedback loop, denoted by the symbol *k*, appeared in the expressions "*-k*ULI" and "-k*DLI"*, which were attached to the two leaky integrators (see Figure 4).

The factor governing the exponential decay of the adapting charge symbolically got placed at the end of the original expression for the adapting charge:

$$\textit{adapting charge} = wx_a(1-e^{-kt_a})(e^{-kt}) \quad (7)$$

where *t* referred to the time spent testing. Following adaptation, the presentation of the stationary test stimulus induced a smaller charge, of RC-circuit type, in the leaky integrators for both directional channels, the forward (adapted) channel and the backward (non-adapted) channel because the stationary test stimulus induced a small non-directional effect:

$$\textit{testing charge} = wx_t(1-e^{-kt}) \quad (8)$$

where x_t referred to the test stimulus. Thus, in the adapted channel, there was the charge built up due to adaptation, the subsequent leaking of the adapting charge during the testing phase, and the small charge built up due to the test stimulus, which collectively were called *u*, with subscripts denoting forward or backward:

$$\textit{adapted channel charge} = u_f(t_s) = [wx_a(1-e^{-kt_a})(e^{-kt})] + [wx_t(1-e^{-kt})]. \quad (9)$$

In the non-adapted channel, there was only the charge built up due to the test stimulus:

$$\textit{non-adapted channel charge} = u_b(t_s) = wx_t(1-e^{-kt}). \quad (10)$$

Adaptation caused the signaling in the adapted channel to become reduced for a period of time; an aftereffect was experienced as long as the difference between signals in the opponent channels was equal to or greater than a given criterion (called θ).

In the Patterson et al. (2009) version of the van de Grind et al. model, there were multiple leaky integrators whose time constants collectively spanned a large range of durations. Multiple integrators were needed to account for the long aftereffects induced by long adaptation durations. The output of the integrators was summed. For the adapted channel, they had:

$$\textit{adapted channel charge} = u_f = \sum_{i=1}^{n}[wx_a(1-e^{-k_i t_a})(e^{-k_i t}) + wx_t(1-e^{-k_i t})], \quad (11)$$

and for the non-adapted channel they had:

$$\textit{non-adapted channel charge} = u_b = \sum_{i=1}^{n}[wx_t(1-e^{-k_i t})], \quad (12)$$

where i = i^{th} mechanism, and n = total number of leaky integrators within each motion-direction channel; in Patterson et al., n = 3. This model entailing multiple continuously-leaking integrator mechanisms per motion-direction channel was called the *'modified van de Grind et al. model'* by Patterson et al.

Turning back to the present MAE data, the modified van de Grind et al. model by Patterson et al. (2009) was used to simulate the present data. It was found that the baseline and central viewing conditions could be approximated by implementing minor modifications to the Patterson et al. *k* factors (e.g., the multiplicative inverse of the time constants) attached to the three leaky integrators, with *k1* = .04662, *k2* = .014, *k3* = .00175. However, for the peripheral viewing condition which showed a faster temporal response, more significant modifications were required, namely a 28.6% increase in the *k* factors (e.g., shorter time constants) relative to the *k* factors established for the baseline and central viewing conditions, such that *k1* = .05994, *k2* = .018, *k3* = .00225 for the peripheral viewing condition.

With these *k* factors, the simulated MAE values (collapsing across the speed variable), compared with the empirical values taken from Figure 3, were as follows: For the average of the baseline and central viewing condition, the simulated MAE duration was 16.25 seconds versus the empirical MAE duration of 16.26 seconds. For the peripheral viewing condition, simulated MAE duration was 12.25 seconds versus the empirical MAE durations of 12.27 seconds. Therefore, for the peripheral viewing condition, the increase in the value of the *k* factors, which translates into shorter time constants, leads to a faster growth rate and faster decay rate in the leaky integrators, which reflects the increased relative speed in the adjustment of the gain control in the peripheral retina, that is, a more transient response for the peripheral retina. Collapsing across viewing condition, the simulated MAE values compared with the empirical values were as

follows: For the average of 20 and 40 eyeheights/sec the simulated duration is 15.75 seconds (*k1* = .044, *k2* = .0176, *k3* = .00132) compared with the empirical value of 15.79 seconds. For the 10 eyeheights/sec condition, the simulated MAE duration is 13.25 seconds (*k1* = .0515, *k2* = .0206, *k3* = .001545) compared with the empirical value of 13.21 seconds.

Turning now to the debate on the peripheral dominance hypothesis versus the central dominance hypothesis, discussed in the Introduction, recall that many authors have posited that the sense of self-motion, as well as other forms of body orientation and alignment, is primarily mediated by stimulation in the peripheral visual field. Early research on circular vection (Brant, Dichgans, & Koenig, 1973), linear and roll vection (Held, Dishgans, & Bauer, 1975; Berthoz, Pavard, & Young, 1977), and postural adjustments (Lestiene, Soechting, & Berthoz, 1977) suggested that the peripheral visual field played a strong role in the perception of self-motion and body orientation. However, recent research has demonstrated that the sense of self-motion, as well as other forms of body orientation and alignment, may be stronger with stimulation of the central visual field. More recent research on circular vection (Howard & Heckman, 1989), linear vection (Anderson, 1986; Andersen & Braunstein, 1985), postural adjustments (Palus, Straube, & Brandt, 1984) and heading judgments (Warren, 1992) suggests that the central visual field was dominant in the perception of self-motion and body orientation.

It is difficult to make sense out of this conflicted literature because these studies employed different definitions of central versus peripheral stimulation and thus utilized a wide variety of different eccentricities when implementing their peripheral stimulation. Moreover, and perhaps more seriously for comparison purposes, these studies employed different dependent variables for measuring the effects of peripheral versus central stimulation, such as magnitude

measures versus angular measures, which prevents the studies from being directly comparable to one another and to the present SRW optic flow MAE study.

Studies of the motion aftereffect using simple adapting patterns have also found conflicting evidence in terms of the influence of stimulation in the central versus peripheral visual field. Recall that O'Shea et al. (1994) revealed that the MAE magnitude induced in the central visual field was greater than that induced in the peripheral visual field. The stimulus used in this study was a spiral pattern configured as a small circular disk with a diameter of 2.8 degrees, or a larger annulus with internal diameter of 40 degrees and external diameter of 80 degrees. However, Castet, Keeble, and Verstraten (2002) and Price, Greenwood, and Ibbotson (2004) found that the magnitude of the MAE was stronger with a peripheral stimulus as compared with a central stimulus. Castet et al. had observers adapt to dynamic random-dot stimuli using a 4 x 4 square degree aperture located at an eccentricity of 0, 4, or 7 degrees. Price et al. had participants adapt to a spiral pattern that was either a small central annulus (inner radius 0.5 degrees and outer radius 5 degrees) or a larger annulus (inner diameter 5 degrees and an outer diameter 7 degrees).

Here again, it is difficult to make sense out of this conflicted literature because these studies employed different definitions of central versus peripheral stimulation and thus utilized different eccentricities when implementing their peripheral stimulation. Indeed, Warren (1992) and O'Shea et al. (1994) have attributed differences in the results among various studies of the MAE to the lack of consistency in the choice of eccentricity of the adapting stimulus. Importantly, the central and peripheral areas in these studies were not equated for cortical magnification and thus were not comparable to one another.

In the present study, the central versus peripheral stimuli were scaled for cortical magnification, which is most appropriate given that motion information is processed at cortical levels of the visual system in humans (Blake & Sekuler, 2005). Thus far, there is only one MAE study (Murakami & Shimojo, 1995) that considered cortical magnification. For the condition with the stimulus size closest to our own (e.g., their largest stimulus size was an area of approximately 10.89 square degrees), there was a trend for increased eccentricity to produce an increase in MAE magnitude as measured by increased cancellation velocity. However, it is difficult to compare the results of Murakami and Shimojo to the present results because it is unknown how MAE cancellation velocity relates to MAE duration. The problem with testing for the magnitude of an MAE with dynamic test stimuli (as Murakami and Shimojo did) is that a faster aftereffect (higher velocity) does not necessarily imply a longer aftereffect (Pantle, 1998).

The present results showing that the peripheral SRW optic flow MAE can be modeled by shortening the time constants of the integrator mechanisms is generally consistent with known properties of the peripheral retina. That is, the central retina is known to have relatively sluggish responding and poor temporal acuity, whereas the peripheral retina possesses a faster, transient response and high temporal acuity (*e.g.*, Livingstone & Hubel, 1988; Milner & Goodale, 1995; Schiller, Logothetis, & Charles, 1990). Apparently this differential responding in the time domain of the central versus peripheral retina is reflected in our SRW optic flow MAE. Finally, the fact that the intermediate and fastest adapting speeds produced the longest MAE durations in the present study is a result that is inconsistent with studies of the MAE using random-dot arrays (*e.g.*, Wohlgeuth, 1911; Thompson, 1993) in that those studies showed that maximal MAE duration occurs with moderate adapting speed. Apparently, a different relationship may occur between adapting speed and MAE duration when simulated self-motion is used as the adaptation

stimulus. However, more data would need to be collected across a greater range of adapting speeds to make definitive statements about the relationship.

REFERENCES

Andersen, G. J. (1986) Perception of self-motion: psychophysical and computation approaches. *Psychological Bulletin,* 99, 52-65.

Andersen, G. J., & Braunstein, M.L. (1985) Induced self-motion in central vision. *Journal of Experimental Psychology: Human Perception & Performance,* 11, 122-132.

Bex, P. J., Metha, A. B., & Makous, W. (1999) Enhanced motion aftereffect for complex motions. *Vision Research,* 39(13), 2229-2239.

Blake, R. & Sekuler, R. (2005) *Perception*. McGraw-Hill Higher Education, New York, NY.

Brant, T., Dichgans, J., & Koenig, E. (1973) differential effects of central versus peripheral vision on egocentric and exocentric motion perception. *Experimental Brain Research,* 16, 476-491.

Bremmer, F. (2005). Navigation in space-the role of the Macaque ventral intraparietal area. *Journal of Physiology, 566,* 29-35.

Bremmer, F., Duhamel, J-R., Ben Hamed, S. & Graf, W. (2002). Heading encoding in the Macaque ventral intraparietal area (VIP). *European Journal of Neuroscience, 16,* 1554-1568.

Bremmer, F., Duhamel, J-R., Ben Hamed, S. & Graf, W. (1997). The representation of movement in near extra-personal space in the Macaque ventral intraparietal area (VIP). In P. Thier and H-O. Karnath (Eds.), Parietal Lobe Contributions to Orientation in 3D Space (pp. 619-630). Heidelberg: Springer-Verlag.

Burke, D. & Wenderoth P. (1993) Determinants of two-dimensional motion aftereffects induced by simulatenously- and alternately-presented plaid components. *Vision Research,* 33, 351-359.

Castet, E., Keeble, D. R. T., & Verstraten, F. A. J. (2002) Nulling the motion aftereffect with dynamic random-dot stimuli: limitations and implications. *Journal of Vision*, 2(4), 302-311.

Cavanagh, P. & Favreau, O. E. (1980) Motion aftereffect: a global mechanism for the perception of rotation. *Perception*, 9, 175-182.

Chaudhuri, A. (1990) Modulation of the motion aftereffect by selective attention. *Nature,* 344, 60-62.

Cowey A. & Rolls E. T. (1974) Human cortical magnification factor and its relation to visual acuity. *Experimental Brain Research,* 21, 447-454.

Dow B. M., Snyder R. G., Vautin R. G. & Bauer R. (1981) Magnification factor and receptive field size in foveal striate cortex of the monkey. *Experimental Brain Research*, 44, 213-228.

Gibson, J. J. (1937) Adaptation with negative aftereffect. *Psychological Review*, 44, 222-244.

Granit, R. (1928) On inhibition in the aftereffect of seen movement. *British Journal of Psychology*, 19, 147.

Held, R., Dichgans, J., & Bauer, J. (1975) Characteristics of moving visual scenes influencing spatial orientation. *Vision Research,* 15, 357-365.

Howard, I. P., & Heckmann, T. (1989) Circular vection as a function of the relative sizes, distances, and positions of two competing visual displays. *Perception*, 18, 657-665.

Lestienne, F., Soeching, J., & Berthoz, A. (1977) Postural readjustments induced by linear motion of visual scenes. *Experimental Brain Research*, 28, 363-384.

Lankheet, M.J.M., van Wezel, R.J.A., & van de Grind, W.A. (1991) Effects of Background Illumination on Cat Horizontal cell Responses. *Vision Research*, 31(6), 919-932.

Levi, D. M. & Aitsebaomo, A. P. (1985) Vernier acuity, crowding and cortical magnification. *Vision Research*, 28(7), 963-977.

Livingstone, M. & Hubel, D. (1988) Segregation of form, color, and depth: anatomy, physiology, and perception. *Science*, 240(4853), 740-749.

Milner, A.D. & Goodale, M.A. (1995) *The visual brain in action.* Oxford: Oxford University Press.

Murakami, I. & Shimojo, S. (1995) Modulation of motion aftereffect by surround motion and its dependence on stimulus size and eccentricity. *Vision Research*, 35(13), 1835-1844.

Nishida, S. & Sato, T. (1995) Motion aftereffect with flickering test patterns reveals higher stages of motion processing. *Vision Research*, 35, 477-490.

O'Shea, R. P., McDonald, A. A., Cumming, A., Peart, D., Sanderson, G, & Molteno A. C. (1994) Interocular transfer of the movement aftereffect in central and peripheral vision of people with strabismus. *Investigative Opthamology & Visual Science*, 35, 313-317.

Pantle, A. (1974) Motion aftereffect magnitude as a measure of the spatio-temporal response properties of direction-selective analyzers. *Vision Research*, 14, 1229-1236.

Pantle, A. (1998) How do measures of the motion aftereffect measure up?. G. Mather, F. Verstraten, and S. Anstis (Eds.) *The Motion Aftereffect* (pp. 25-39). The MIT Press: Cambridge, MA.

Patterson, R., Fournier, L. R., Wiediger, M., Vavrek, G., Becker-Dippman, C., & Bickler, I. (2005) Selective attention and cyclopean motion processing. *Vision Research, 45(20),* 2601-2607.

Patterson R., Tripp, L., Rogers, J., & Boydstun, A. (2009) Modeling the simulated real world optic flow motion aftereffect. *Journal of the Optical Society of America A*, in press.

Patterson R., Winterbottom, M., & Pierce, B. (2006) Perceptual issues in the use of head-mounted visual displays. *Human Factors, 48(3),* 555-573.

Paulus, W. M., Straube, A., & Brant, T. (1984) Visual stabilization of posture: Physiological stimulus characteristics and clinical aspects. *Brain*, 107, 1143-1163.

Price, S. C., Greenwood, J. A., & Ibbotson, M. R. (2004) Tuning properties of radial phantom motion aftereffects. *Vision Research*, 44, 1971-1979.

Rovamo J., Virsu V., & Nasanen, R. (1978) Cortical magnification factor predicts the photopic contrast sensitivity of peripheral vision. *Nature*, 271, 54-56.

Schiller, P.H., Logothetis, N.K., & Charles, E.R. (1990) Role of the color-opponent and broad-band channels in vision. *Visual Neuroscience*, 5(4), 321-346.

Scott, T. R. & Noland, J. H. (1965) Some stimulus dimensions of rotating spirals. *Psychological review*, 72, 344-357.

Thompson, P. (1993) Motion psychophysics. In *Visual Motion and Its Role in the Stabilization of Gaze*, Ed. J. Wallman and F. A. Miles. Amsterdam, Elsvier, pp.29-52.

Virsu V. & Rovamo J. (1979) Visual resolution, contrast sensitivity, and the cortical magnification factor. *Experimental Brain Research*, 37, 475-494.

van de Grind, W.A., Lankheet, M.J.M. & Tao, R. (2003). A gain-control model relating nulling results to the duration of dynamic motion aftereffects. *Vision Research*, 43, 117-133.

van de Grind, W.A., van der Smagt, M.J. & Verstraten, F.A.J. (2004). Storage for free: a surprising property of a simple gain-control model of motion aftereffects. *Vision Research*, 44, 2269-2284.

Warren, W. H. (1992) The role of central and peripheral vision in perceiving the direction of self-motion. *Perception & Psychophysics*, 51(5), 443-454.

Warren, W. H., (1998). *The state of flow*. Cambridge, MA, US: The MIT Press.

Wohlgemuth, A. (1911) On the after-effect of seen movement. *British Journal of Psychology*, 1, 1-117.

APPENDIX

Figure 1: Picture of the visual display showing a simulated real-world scene. In the study, the sky was light blue and the ground plane a homogeneous gray.

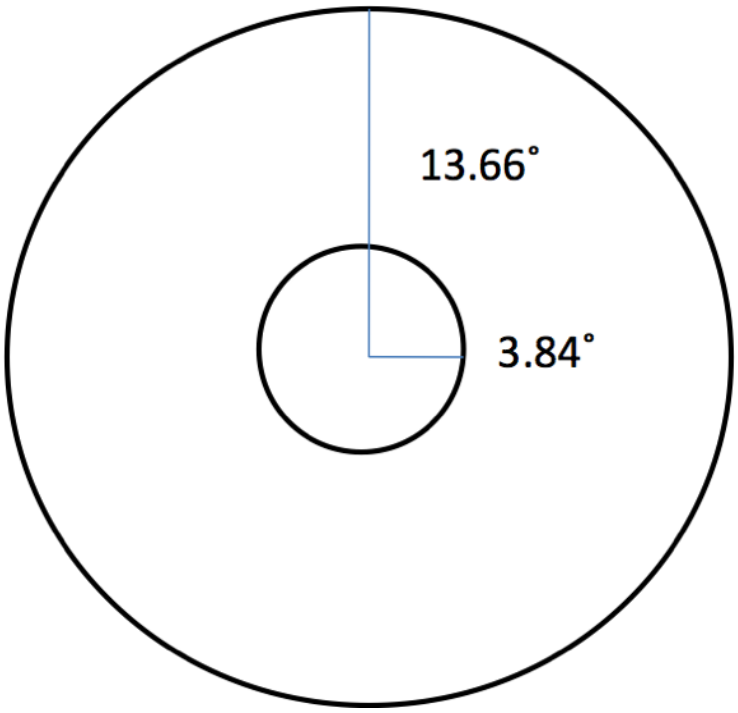

Figure 2: Diagram depicting the angular dimensions of the adapting and test stimuli used in the study. The central visual field condition consisted of the display being masked off except for the center disk which had a radius of 3.84 degrees (area = 46.30 square degrees). The peripheral visual field consisted of the display being masked off except for a surrounding annulus whose dimension measured 3.84 degrees (inner edge) and 13.66 degrees (outer edge) (area = 540.01 square degrees). Note that these areas were consistent with a normalization procedure based on cortical magnification.

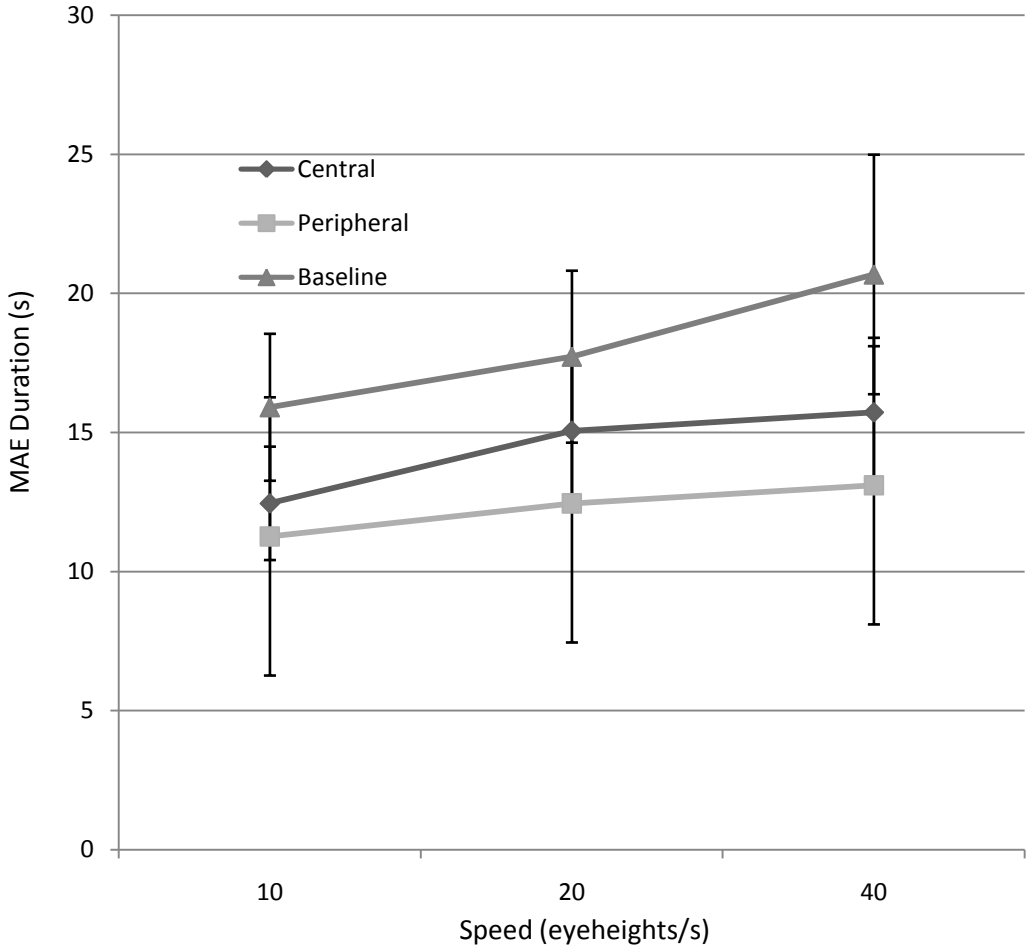

Figure 3: MAE duration (ordinate) for three speeds of self-motion (e.g., global optical flow rate; abscissa) and three viewing conditions (legend). Each data point is the mean of 11 observers. Each error bar represents plus or minus 1 standard error of the mean.

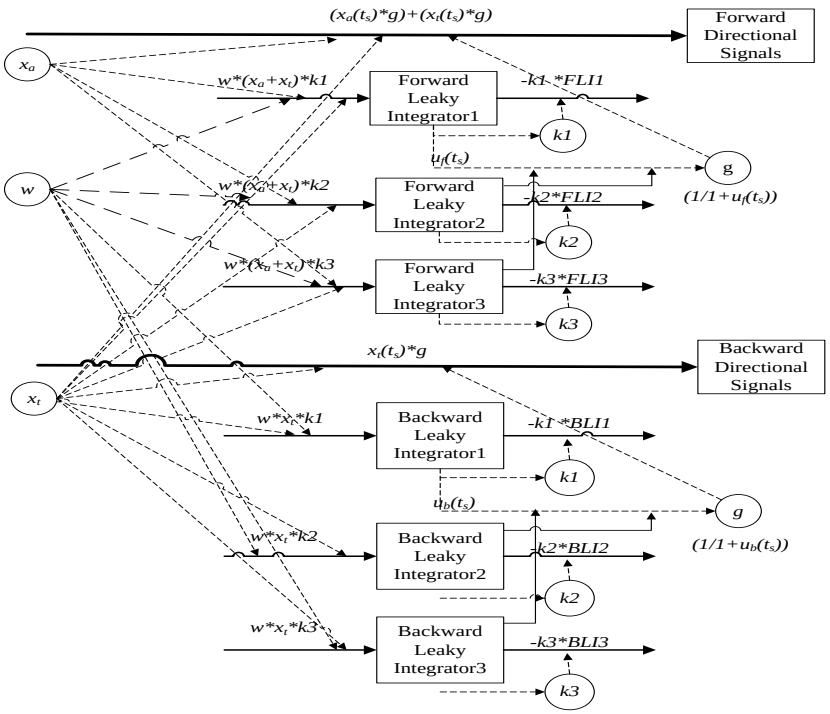

Figure 4: A system dynamics representation of the SRW optic flow MAE model by Patterson, Tripp, Rogers, and Boydstun, 2009. This model is a multiple-mechanism self-motion model based on the van de Grind et al. (2003, 2004) model. Rectangles (stocks) represent integration, solid arrows (flows) represent rates of change or derivatives, dashed arrows represent information connections and feedback, and circles represent variables or operations. Information processing flows from left to right. The two solid thick horizontal arrows represent signals in the forward and backward self-motion direction channels, respectively. xa and xt are the adaptation stimulus and test stimulus, respectively; w is a weighting constant. The six stocks in the middle of the diagram represent leaky integrators in the model, three integrators for the forward-direction channel ("Forward Leaky Integrator") and three integrators for the backward-direction channel ("Backward Leaky Integrator"). The gain in each of the channels is denoted by the symbol g. kn is the inverse of the time constant of the negative feedback loop (e.g., "-k1*FLI1")

on each leaky integrator, where n = 1, 2, or 3. Computations performed in the simulation are shown above or below their respective icons.